

Effects of self- and cross-phase modulation on photon purity for four-wave-mixing photon pair sources

Bryn Bell,^{1,2,*} Alex McMillan,¹ Will McCutcheon,¹ and John Rarity¹

¹*Department of Electrical and Electronic Engineering, University of Bristol, Bristol BS8 1UB, United Kingdom*

²*Centre for Ultrahigh bandwidth Devices for Optical Systems (CUDOS), Institute of Photonics and Optical Science (IPOS),*

School of Physics, University of Sydney, Sydney, NSW 2006, Australia

(Received 14 April 2015; published 20 November 2015)

We consider the effect of self-phase modulation and cross-phase modulation on the joint spectral amplitude of photon pairs generated by spontaneous four-wave mixing. In particular, the purity of a heralded photon from a pair is considered in the context of schemes that aim to maximize the purity and minimize correlation in the joint spectral amplitude using birefringent phase matching and short pump pulses. We find that nonlinear phase-modulation effects will be detrimental and will limit the quantum interference visibility that can be achieved at a given generation rate. An approximate expression for the joint spectral amplitude with phase modulation is found by considering the group velocity walk-off between each photon and the pump but neglecting the group-velocity dispersion at each wavelength. The group-velocity dispersion can also be included with a numerical calculation, and it is shown that it has only a small effect on the purity for the realistic parameters considered.

DOI: [10.1103/PhysRevA.92.053849](https://doi.org/10.1103/PhysRevA.92.053849)

PACS number(s): 42.65.Lm, 42.50.Dv, 03.67.Bg

I. INTRODUCTION

Single-photon sources are a vital component of developing quantum technologies such as quantum cryptography [1], linear optical quantum computing [2], and quantum metrology [3], and improved sources need to be developed to enable these applications. In addition to requiring high-efficiency, on-demand single photons, many applications require that the photons be generated in a single mode, with well-defined spatial characteristics and a Fourier-transform-limited spectral-temporal shape. This allows two separate photons to be indistinguishable and to undergo high-quality quantum interference [4]; this, in turn, makes possible fundamental operations such as teleportation of the photon [5] and two-photon logic gates [6].

Photon pairs generated in a nonlinear medium by spontaneous parametric downconversion (SPDC) or four-wave mixing (FWM) are often used as a source of single photons, with one of the photons detected to give a heralding signal, indicating the presence of the other [7,8]. Although this method is inherently nondeterministic, through the multiplexing of many such sources and the use of active switching, it is, in principle, possible to construct a source arbitrarily close to a deterministic source [9,10]. However, the photons of a pair are generally correlated in frequency or time, which means that the single photons will arrive in a statistical mix of multiple modes. Narrow spectral filtering of the single photons can force them into a single mode but at a cost to the overall transmission and heralding efficiency, which reduces the usefulness of the source. Possible solutions to this problem have been demonstrated based on consideration of the joint spectral amplitude (JSA) of a pair: with careful choice of wavelengths or by engineering the dispersion properties of the nonlinear medium, the degree of correlation can be minimized, allowing quantum interference to take place without narrow filtering [11]. For SPDC in bulk crystals interference visibilities as

high as 94.5% have been observed without filtering [12]. For FWM in birefringent optical fibers unfiltered visibilities have tended to fall short of theoretical estimates, often in the range 70%–80%, which is far from sufficient for scalable use in communications or computing [13–16]. It has been suggested that inhomogeneity along the length of fibers due to fabrication imperfections is responsible for the shortfall in visibility, and it has been shown theoretically that a large inhomogeneity can reduce the visibility [17]. However, it is also expected to create a broadening and modulation in the spectra of the individual photons, which should be easily detected, and in some situations a small amount of inhomogeneity could actually improve the interference visibility [18].

Here, we consider the effects of parasitic nonlinear processes on the JSA and the interference visibility, namely, self-phase modulation (SPM) and cross-phase modulation (XPM), which are not present in a $\chi^{(2)}$ nonlinear medium such as the crystals used for SPDC but are potentially significant in a $\chi^{(3)}$ nonlinearity such as fiber [19]. Previous calculations of the JSA have tended to account for SPM and XPM in a simplistic form which is only exact in a continuous-wave (cw) regime, whereas the relevant schemes to make the JSA uncorrelated rely on the use of short pulses. We show that these effects can cause a reduction in interference visibility, especially when a source is operated at a high pair generation rate, beginning from an analytic explanation then progressing to a numerical model fully accounting for SPM, XPM, and dispersion.

II. JOINT SPECTRAL AMPLITUDES

In pair production through FWM, a bright pump laser is used to power the process. As the pump pulse propagates through a $\chi^{(3)}$ medium, two pump photons may be spontaneously annihilated, with a correlated signal-idler photon pair created. The frequencies of the signal and idler are constrained by the conservation of energy and momentum:

$$\begin{aligned}\Delta\omega &= 2\omega_p - \omega_s - \omega_i = 0, \\ \Delta\beta &= 2\beta_p - \beta_s - \beta_i + (2\gamma_p - 2\gamma_s - \gamma_i)P = 0.\end{aligned}\tag{1}$$

*bbell@physics.usyd.edu.au

$\omega_{p,s,i}$ refer to the frequencies of pump, signal, and idler and $\beta_{p,s,i}$ refer to the wave vectors. The $\gamma_{p,s,i}P$ terms arise from SPM and XPM, as the intense pump in the nonlinear medium will slightly modify the wave vectors, with $\gamma_{p,s,i}$ being effective nonlinear coefficients for pump, signal, and idler and P being the peak power of the pump.

These conditions are not exact, and the photons will have some bandwidth centered on an exact solution. The finite bandwidth of the pump will introduce some uncertainty to the $\Delta\omega$ condition, and for a fiber of finite length, there is some uncertainty in the phase matching which permits small values of $\Delta\beta$. The JSA can be simply expressed as the product of an energy-matching and a phase-matching function [11,20]:

$$\mathcal{A}_{\text{spec}}(\omega_s, \omega_i) = F \times G, \quad (2)$$

with $\mathcal{A}_{\text{spec}}$ the JSA function and with

$$F = \iint d\omega_{p1} d\omega_{p2} E(\omega_{p1}) E(\omega_{p2}) \delta(\omega_{p1} + \omega_{p2} - \omega_s - \omega_i), \quad (3)$$

$$G = e^{i\Delta\beta L/2} \text{sinc}\left(\frac{\Delta\beta L}{2}\right). \quad (4)$$

Here, $E(\omega)$ is the spectral amplitude of the pump, and the two pump photon frequencies ω_{p1} and ω_{p2} are integrated over. It can usually be assumed that the two are approximately equal; then F is just the convolution of $E(\omega)$ with itself, and the δ function, which results from energy conservation, fixes $\omega_p = (\omega_s + \omega_i)/2$. For instance, if the pump amplitude is a Gaussian, $E(\omega_p) = E_0 e^{-\frac{(\omega_p - \omega_{p0})^2}{2\sigma^2}}$, then

$$F = E_0^2 e^{-\frac{(\omega_s + \omega_i - 2\omega_{p0})^2}{16\sigma^2}}. \quad (5)$$

Another useful simplification is to consider the different group velocities at the pump, signal, and idler frequencies but ignore higher-order dispersion terms. Then, for small departures from an exactly phase matched solution $\Delta\omega_s$ and $\Delta\omega_i$, the phase mismatch can be expressed as

$$\Delta\beta = \Delta\omega_s(\beta_{1p} - \beta_{1s}) + \Delta\omega_i(\beta_{1p} - \beta_{1i}) - 2\gamma P, \quad (6)$$

with $\beta_{1m} = d\beta/d\omega_m = 1/v_g$, one over the group velocity at each frequency, $m = p, s, i$. It can be seen that the differences in $1/v_g$ between pump, signal, and idler are an important factor in determining the JSA and its degree of correlation, or its factorability. Figure 1 shows three JSAs calculated approximately in this fashion. In Fig. 1(a), the group velocities are chosen arbitrarily with $\beta_{1p} > \beta_{1i} > \beta_{1s}$, resulting in a highly correlated JSA. In Fig. 1(b), the idler is group velocity matched to the pump, resulting in an uncorrelated JSA, as the main peak now has its axes horizontal and vertical, although the ripples to either side, resulting from the sinc function in G , remain correlated. This is the asymmetric scheme to generate a factorable JSA [13]. In Fig. 1(c), β_{1s} and β_{1i} are roughly equally spaced above and below β_{1p} , the symmetric scheme for a factorable JSA [16]. Here, the bandwidth of the pump must be exactly tuned to make the main peak circular in shape and uncorrelated. The conditions on the group velocities are generally met by using birefringent phase matching, with the

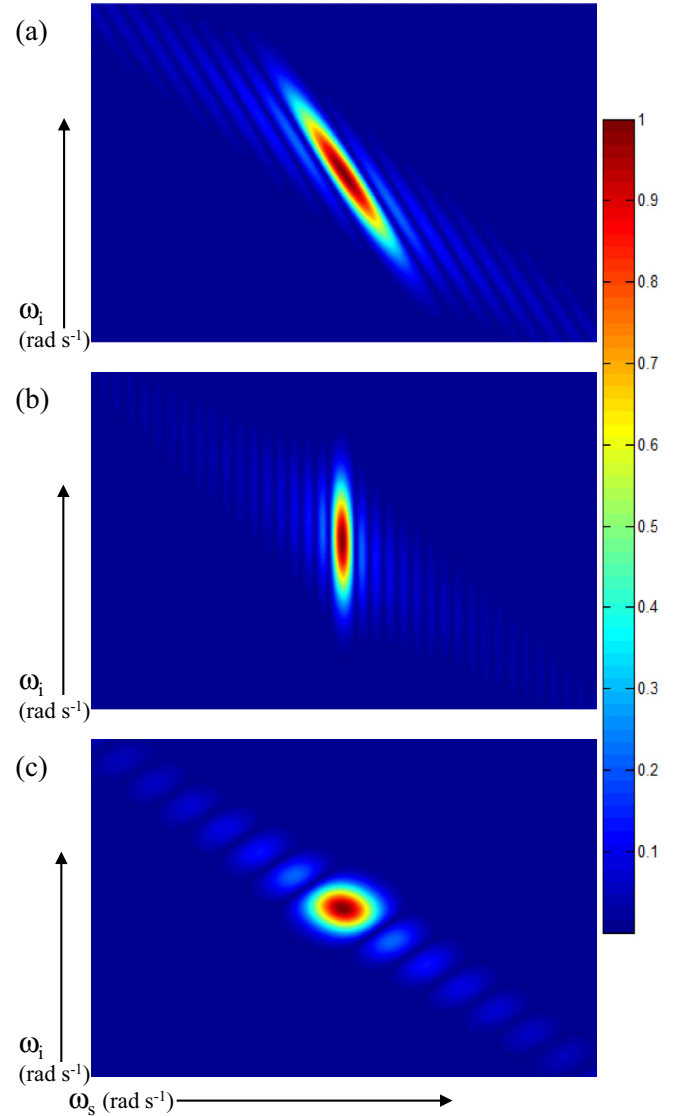


FIG. 1. (Color online) Joint spectral amplitudes calculated simply from the pump, signal, and idler group velocities. (a) General example with $\beta_{1p} > \beta_{1i} > \beta_{1s}$ results in a highly correlated signal and idler, indicated by the diagonal nature of the main peak, (b) $\beta_{1p} = \beta_{1i}$ results in the central peak becoming vertical and uncorrelated, and (c) when $\beta_{1p} - \beta_{1s} \approx \beta_{1i} - \beta_{1p}$, the phase-matching condition lies at $+45^\circ$ while the energy matching lies at -45° . Tuning the pump bandwidth can make the central peak circular and uncorrelated. All JSAs are plotted as absolute values, ignoring the complex phase, and are shown normalized to have a maximum of 1.

pump polarized on the slow birefringent axis and the photons on the fast axis.

For a given JSA, the degree of correlation can be calculated using the singular value decomposition function in MATLAB. This provides a Schmidt decomposition of the JSA:

$$\mathcal{A}_{\text{spec}}(\omega_s, \omega_i) = \sum_j \lambda_j f_j(\omega_s) g_j(\omega_i), \quad (7)$$

where $f_j(\omega_s)$ and $g_j(\omega_i)$ are a set of orthogonal spectral modes for signal and idler and λ_j are real amplitude coefficients. We

define the purity as

$$P = \sum_j \lambda_j^4, \quad (8)$$

which is an upper limit on the quantum interference visibility possible between two photons from separate pairs [21].

For the JSAs in Fig. 1, the purities are found to be 23% for the correlated JSA in Fig. 1(a), 95% for the asymmetric uncorrelated case in Fig. 1(b), and 83% for the symmetric case in Fig. 1(c). In Fig. 1(c), the purity is mainly limited by the correlation in the sinc function ripples to either side of the main peak. These can be removed by filtering, resulting in high purities with relatively little cost to transmission efficiency [16].

The nonlinear correction $-2\gamma P$ to $\Delta\beta$, which has been ignored in the calculations above, depends on the pump power. For a pulsed pump, P is a function of position and time and cannot be simply expressed in the frequency domain; previously, the peak power has been used. Instead, we take SPM and XPM into account by working in the time domain and developing expressions for the joint temporal amplitude (JTA), which is linked to the JSA by two-dimensional (2D) Fourier transform.

III. EQUATIONS OF MOTION IN A NONLINEAR FIBER

To model photon pair production through FWM with SPM and XPM included exactly, we use the equations of motion with position and time for the pump, signal, and idler fields in a $\chi^{(3)}$ medium. The electric field associated with the pump pulse can be split into positive and negative frequency components as

$$\mathbf{E} = \mathbf{e}X(x, y)(E_p^+ e^{i(\beta_{p0}z - \omega_{p0}t)} + E_p^- e^{-i(\beta_{p0}z - \omega_{p0}t)}). \quad (9)$$

Here, \mathbf{e} is the polarization vector of the electric field. $X(x, y)$ is the transverse mode shape, normalized such that $\iint X(x, y)^2 dx dy = 1$. Complex oscillatory terms have been separated out at a central frequency ω_{p0} and wave vector β_{p0} . This leaves E_p^+ as a complex envelope function describing the pulse, dependent on time t and position z along the propagation axis z . E_p^- is the complex conjugate of E_p^+ .

Assuming the pulse envelope varies slowly (the length of the pulse contains many optical cycles, or equivalently, the bandwidth of interest is small compared to the frequency ω_{p0}) and that the nonlinearity is a small perturbation to the linear evolution of the pulse, E_p^+ obeys the nonlinear Schrödinger equation [22]:

$$\frac{\partial E_p^+}{\partial z} + \beta_{1p} \frac{\partial E_p^+}{\partial t} + \frac{i\beta_{2p}}{2} \frac{\partial^2 E_p^+}{\partial t^2} = i\gamma_p |E_p^+|^2 E_p^+. \quad (10)$$

The β_{1p} term corresponds to the group velocity of the pump pulse. In the following it is removed from the equation as we consider all quantities in a moving reference frame. The β_{2p} term gives rise to dispersion; higher-order dispersion terms are neglected here but can be included as higher-order time derivatives. The term on the right-hand side is the nonlinearity associated with SPM of the pump, with $\gamma_p = \gamma(\omega_{p0})$ being an

effective nonlinear coefficient:

$$\gamma(\omega) = \frac{3\chi^{(3)}\omega}{2cn_\omega A}, \quad (11)$$

where n_ω is the refractive index at the frequency ω and A is the effective area of the transverse mode.

Analogous equations of motion for the signal and idler fields can be written as

$$\frac{\partial E_s^+}{\partial z} + \beta_{1s} \frac{\partial E_s^+}{\partial t} + \frac{i\beta_{2s}}{2} \frac{\partial^2 E_s^+}{\partial t^2} = i\gamma_s (2|E_p^+|^2 E_s^+ + E_p^{+2} E_i^-), \quad (12)$$

$$\frac{\partial E_i^+}{\partial z} + \beta_{1i} \frac{\partial E_i^+}{\partial t} + \frac{i\beta_{2i}}{2} \frac{\partial^2 E_i^+}{\partial t^2} = i\gamma_i (2|E_p^+|^2 E_i^+ + E_p^{+2} E_s^-). \quad (13)$$

In the moving reference frame, β_{1s} and β_{1i} are taken to be group velocity terms relative to the pump (i.e., $\beta_{1s} \rightarrow \beta_{1s} - \beta_{1p}$ and $\beta_{1i} \rightarrow \beta_{1i} - \beta_{1p}$). The first term on the right-hand side of these equations is XPM, as the pump modifies the refractive index experienced by the signal and idler. The second term relates to FWM, with the strong pump field creating a coupling between the signal and idler fields. For simplicity, the central frequencies of the signal and idler have been chosen to be a point of exact phase matching with the central frequency of the pump, so that

$$\begin{aligned} 2\omega_{p0} - \omega_{s0} - \omega_{i0} &= 0, \\ 2\beta_{p0} - \beta_{s0} - \beta_{i0} &= 0. \end{aligned} \quad (14)$$

Note that since the pump field is many orders of magnitude brighter than the signal and idler, which on average will contain less than one photon, terms representing SPM of the signal and idler and XPM from the signal or idler to other fields are ignored. Similarly, depletion of the pump due to FWM is neglected.

The $\chi^{(3)}$ coefficient will generally be three times smaller in nonlinear effects coupling fields of orthogonal polarization compared to fields which are all copolarized [22]. In the birefringent phase-matching schemes considered, the signal and idler are orthogonally polarized to the pump, so this is incorporated by defining $\gamma_s = \gamma(\omega_{s0})/3$ and $\gamma_i = \gamma(\omega_{i0})/3$.

Although the pump laser can continue to be treated classically, the signal and idler fields should be quantized. We use the following quantization, similar to [23,24]:

$$\hat{E}_s^+ = \int d\omega \sqrt{\frac{\hbar\omega}{4\pi\epsilon_0 cn_\omega}} \hat{a}_\omega e^{-i(\beta_{s0}z + \omega t - \omega_{s0}t)}, \quad (15)$$

where \hat{a}_ω are annihilation operators for a photon at position z with frequency ω , with Hermitian conjugate creation operators \hat{a}_ω^\dagger . An identical expression applies to the idler, with the integral taken to be over a different range of frequencies, so that the two remain distinct. The frequency modes are continuous, so the creation and annihilation operators have a commutation relation $[\hat{a}_\omega, \hat{a}_{\omega'}^\dagger] = \delta(\omega - \omega')$, and the number density operator $\hat{a}_\omega^\dagger \hat{a}_\omega$ should be integrated over a frequency interval in order to refer to the actual number of photons within that interval.

It is convenient to consider the signal and idler in terms of the creation and annihilation operators for a photon at a

particular time and position, $\phi^\dagger(z, t)$ and $\phi(z, t)$, which are the Fourier transforms (from frequency to time) of \hat{a}_ω^\dagger and \hat{a}_ω . If the frequencies of interest for the signal and idler lie in a narrow bandwidth about ω_{s0} and ω_{i0} , the electric fields have a simple approximate relation to the new operators:

$$\hat{E}_s^+ = \sqrt{\frac{\hbar\omega_{s0}}{2\epsilon_0 c n_s}} \phi_s, \quad \hat{E}_i^+ = \sqrt{\frac{\hbar\omega_{i0}}{2\epsilon_0 c n_i}} \phi_i. \quad (16)$$

Like $\hat{E}_{s,i}^+$, $\phi_{s,i}$ have the quickly varying oscillations with z removed.

These equations of motions do not have convenient solutions, even the classical equation for the pump, which is independent of the signal and idler, unless we neglect the dispersion terms β_2 . Fortunately, as above, the purity largely depends on the different group velocities for the pump, signal, and idler, and the approximate solutions ignoring dispersion are still instructive. To include dispersion properly, numerical methods can be used, as described later.

IV. APPROXIMATE SOLUTIONS

Once the β_1 term is removed from Eq. (10) using a moving reference frame and the β_2 term is ignored, the pump pulse will retain its temporal shape as it propagates down the fiber, only accumulating a nonlinear phase due to SPM:

$$E_p^+(z) = E_p^+(0)e^{i\theta_p}, \quad (17)$$

where

$$\theta_p = \gamma_p z |E_p^+(0)|^2. \quad (18)$$

Below, E_p^+ is taken to mean the pump amplitude as a function of time at $z = 0$. The signal and idler equations still include a group velocity term in addition to XPM and FWM terms. In the interaction picture of quantum mechanics, the group velocity and XPM parts of the evolution, which affect signal and idler individually, are applied to the operators, while the FWM interaction between the signal and idler is applied to the wave function $|\psi\rangle$. We first write the solutions $\phi_{s,i}$ to the group velocity and XPM terms, ignoring FWM:

$$\phi_s(z, t) = \phi_s(0, t - \beta_{1s}z)e^{i\theta_s}, \quad (19)$$

where the nonlinear phase acquired due to XPM is

$$\theta_s = \frac{2\gamma_s}{\beta_{1s}} \int_{t-\beta_{1s}z}^t |E_p^+|^2 dt, \quad (20)$$

with an analogous solution for ϕ_i . Note that because the signal (or idler) experiences group-velocity walk-off from the pump, it accumulates phase from the pump at a range of different times, hence the integral. If the signal were group velocity matched to the pump, $\beta_{1s} = 0$, the phase would become $\theta_s = 2\gamma_s z |E_p^+(t)|^2$.

The evolution of the wave function according to FWM is now given by

$$\frac{d}{dz} |\psi\rangle = i\hat{H} |\psi\rangle, \quad (21)$$

with

$$\hat{H} = \sqrt{\gamma_s \gamma_i} \int dt E_p^{+2} \phi_s^\dagger \phi_i^\dagger e^{2i\theta_p} + E_p^{-2} \phi_s \phi_i e^{-2i\theta_p}. \quad (22)$$

Since the pair rate per pulse will generally be small, to avoid multipair emission, we take the interaction to first order, beginning with the signal and idler modes in the vacuum state:

$$|\psi\rangle = |\text{vac}\rangle + i\sqrt{\gamma_s \gamma_i} \iint_0^L dt dz E_p^{+2} \phi_s^\dagger \phi_i^\dagger e^{2i\theta_p} |\text{vac}\rangle, \quad (23)$$

with L being the fiber length. To extract the JTA from this wave function, we take the overlap between $|\psi\rangle$ and a signal-idler pair at times t_s, t_i :

$$\mathcal{A}_{\text{temp}}(t_s, t_i) = \langle \text{vac} | \phi_s(L, t_s) \phi_i(L, t_i) | \psi \rangle. \quad (24)$$

With $\mathcal{A}_{\text{temp}}$ the JTA function. Substituting in Eq. (19) and simplifying, we have, for $\beta_{1s} \neq \beta_{1i}$,

$$\mathcal{A}_{\text{temp}}(t_s, t_i) = \begin{cases} \frac{i\sqrt{\gamma_s \gamma_i}}{\beta_{1s} - \beta_{1i}} e^{i\Theta} E_p^+(t_c)^2 & \text{if } 0 < z_c < L, \\ 0 & \text{otherwise,} \end{cases} \quad (25)$$

with z_c being the point in the fiber at which the pair was created. This is defined for a particular t_s, t_i because the signal and idler must be created at the same time, t_c , and the extent to which they have walked off from each other identifies the length they have propagated through after creation. Similarly, t_c is defined by the differing arrival times of the signal and idler:

$$z_c = L - \frac{t_s - t_i}{\beta_{1s} - \beta_{1i}}, \quad t_c = \frac{\beta_{1s} t_i - \beta_{1i} t_s}{\beta_{1s} - \beta_{1i}}. \quad (26)$$

Θ is the total nonlinear phase, given by

$$2\gamma_p z_c |E_p^+(t_c)|^2 + \frac{2\gamma_s}{\beta_{1s}} \int_{t_c}^{t_s} |E_p^+|^2 dt + \frac{2\gamma_i}{\beta_{1i}} \int_{t_c}^{t_i} |E_p^+|^2 dt. \quad (27)$$

This is the source of the distinguishability arising from phase-modulation effects and is clearly dependent on pump intensity. The first term in this expression for Θ relates to the SPM of the pump. Any phase accumulated by the pump before the pair is generated at z_c is passed on to the photons, increased by a factor of 2 due to the quadratic dependence on the pump field. The second and third terms relate to XPM, affecting the signal and idler, respectively. XPM is accumulated only after the pair is created until the end of the fiber, so the integral is between t_c and $t_{s,i}$. The total probability of generating a pair, or the generation rate per laser pulse, is given by

$$R = \iint |\mathcal{A}_{\text{temp}}|^2 dt_s dt_i = \frac{\gamma_s \gamma_i L}{|\beta_{1s} - \beta_{1i}|} \int |E_p^+|^4 dt, \quad (28)$$

which is proportional to pump intensity squared. When dispersion is included, it will affect R by causing the pump pulse to broaden or compress in time, respectively decreasing or increasing the generation rate. In the following, R is calculated by numerical integration of a JTA over t_s and t_i .

It can be seen that if R is increased by increasing the pump intensity, the nonlinear phase shift Θ will also increase. Similarly, if a larger length L is used to increase R , the nonlinear phase becomes more significant, as both the average value of z_c increases and t_s, t_i will, on average, become further from t_c . In the next two sections, we consider the decrease in P due to the nonlinear phase modulation as R is increased for realistic physical parameters. Plotting P as a function of R means that all factors affecting nonlinearity and the brightness of the FWM are taken into account, allowing fair comparisons

to be made between fibers of different lengths or pump pulses of different durations.

A. Asymmetric scheme

When the idler and pump are group velocity matched, $\beta_{ii} = 0$, $t_c = t_i$. Also the last term in Θ , representing XPM from the pump to idler, becomes

$$2\gamma_i(L - z_c)|E_p^+(t_i)|^2 \quad (29)$$

because there is no walk-off between the pump and idler.

Figure 2 shows the joint temporal amplitude for three different lengths of fiber, with a Gaussian pump shape $E_p^+ \propto e^{-t^2/2\tau^2}$. It can be seen that for short lengths, the photons are highly correlated in time, with hard edges to the JTA due to the

condition $0 < z_c < L$. As the length is increased, the signal walk-off smears out the JTA, making it closer to rectangular and less correlated. The fiber length is not important in itself as much as the ratio between the fiber length and the length of the pump pulse τ , as changing both by a constant factor is simply a rescaling of the JTA. It will appear uncorrelated if $\beta_{1s}L/\tau \gg 1$, although in practice this may be limited by dispersive effects which have been ignored so far since they will become more significant for longer lengths and shorter pulses.

The JTAs are shown as absolute values and so are not affected by the nonlinear phase. The effects can be seen in the JSA obtained by taking the Fourier transform of the JTA; in Fig. 3, the JSA is shown for increasing probability of pair

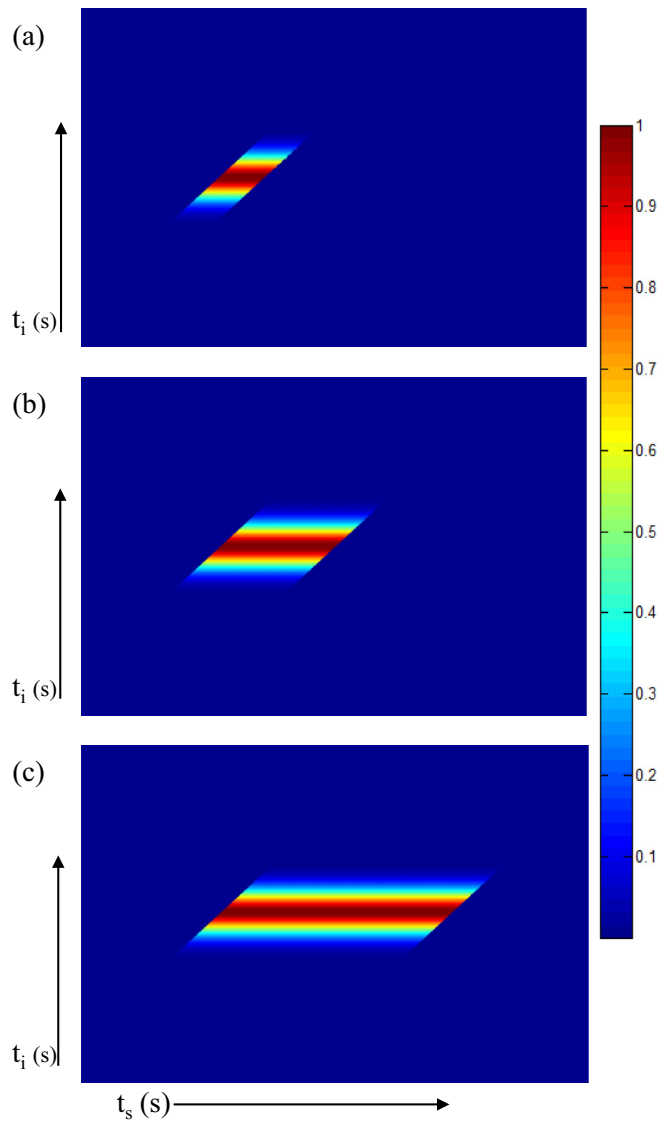


FIG. 2. (Color online) Joint temporal amplitudes when the idler and pump are group velocity matched. For increasing fiber length compared to the length of the pump pulse τ , the group velocity walk-off of the signal smears out the JTA. (a) $\beta_{1s}L/\tau = 2$, (b) $\beta_{1s}L/\tau = 5$, and (c) $\beta_{1s}L/\tau = 10$.

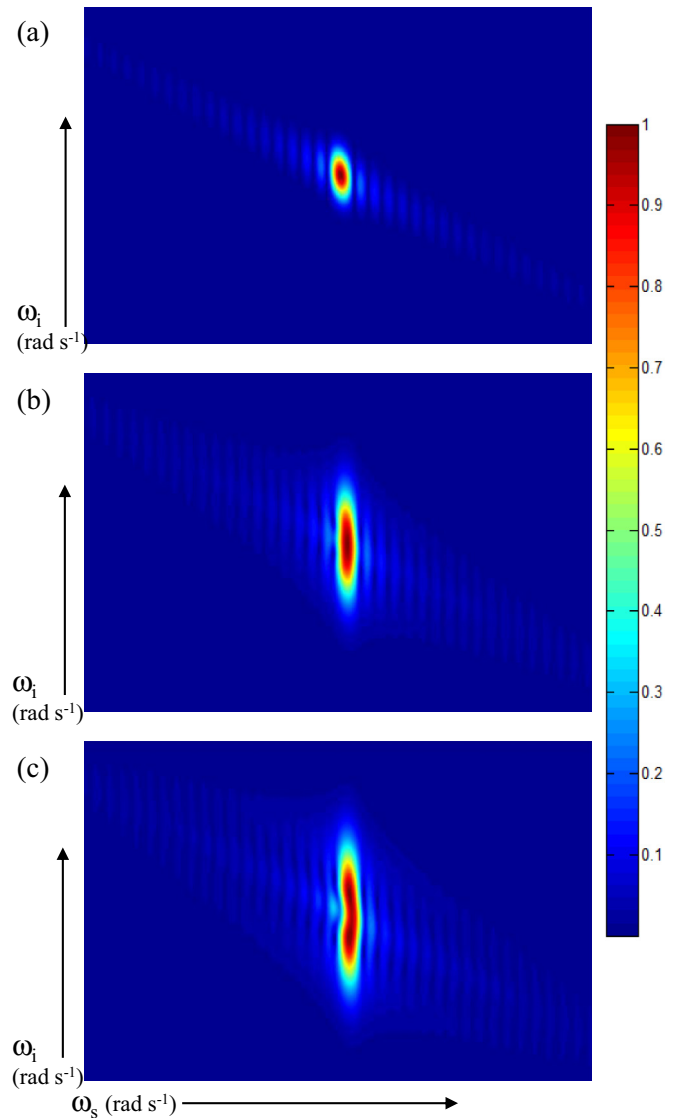


FIG. 3. (Color online) JSA for increasing generation rates R , showing the correspondingly increasing effects of SPM and XPM. The initial effect is to broaden the idler, eventually leading to a splitting and distortion of the JSA which reduces the purity P . (a) R approaching zero, $P = 89\%$. (b) $R = 0.1$, $P = 83\%$. (c) $R = 0.2$, $P = 78\%$.

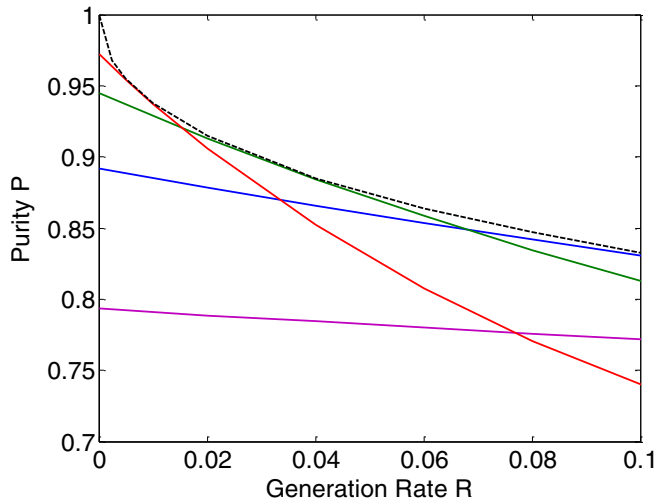


FIG. 4. (Color online) Purity plotted against generation rate for four choices of fiber parameters. As R increases, SPM and XPM become significant and reduce P . Red: $\beta_{1s}L/\tau = 40$. Green: $\beta_{1s}L/\tau = 20$. Blue: $\beta_{1s}L/\tau = 10$. Purple: $\beta_{1s}L/\tau = 5$. The black dashed line shows the purity at a given generation rate after numerical optimization of $\beta_{1s}L/\tau$. It can be seen that a large value of $\beta_{1s}L/\tau$ is desirable at low rates, but for higher rates it will cause a more rapid falloff in purity.

creation R in a pulse, in each case with $\beta_{1s}L/\tau = 10$. As R increases, the idler is broadened significantly by phase modulation and begins to distort in profile. This causes the purity to decrease, from 89% at $R = 0$ to 83% at $R = 0.1$ to 78% at $R = 0.2$ (0.2 pair per pulse may be unrealistically high for an experiment but allows the distortion of the JSA to be seen clearly).

In Fig. 4, the purity is plotted against the pair generation rate R for different choices of fiber parameters. It can be seen that for larger values of $\beta_{1s}L/\tau$, the purity will be high at very low R but will decrease rapidly as R increases, whereas a smaller value of $\beta_{1s}L/\tau$ will decrease more slowly and may be optimal for a given R . Note that, even after optimizing the purity with the fiber parameters, the purity will be more detrimental to quantum interference quality than multipair emission over the range shown, $0 < R \leq 0.1$. (The probability of multipair emission is estimated as R^2 , which, when compared to the rate of single-pair emission R , can reduce the interference visibility by at most R .) This is potentially significant if the end goal is to build a deterministic photon source by multiplexing together many of these sources [9], then to achieve high-quality interference without filtering for quantum communication or computing applications. It is usually assumed that the end quality will be high as long as multipair emission is kept low from the individual sources, but this shows that, at least for this asymmetric scheme using FWM, the effects of phase modulation are likely to be the limiting factor for the generation rate.

Inspection of Eq. (27) does suggest a solution to this problem. The nonlinear phase factor $e^{i\phi}$ becomes a factorable function of t_s and t_i over the extent of the JTA as long as the pump field E_p^+ is a square function in time. The phase is correlated only because $|E_p^+(t_c)|^2$ varies across the JTA.

However, the effects of group-velocity dispersion acting on a short, square pulse over a large length may be unpleasant. Using realistic dispersion parameters based on the birefringent microstructured fiber in [25,26] with a length 50 cm and calculating the JSA from Eq. (2), without phase-modulation effects, the maximum value of P using a square pulse of optimal duration is found to be 80%. Prechirping the pulse to compensate the dispersion so that it is square at the midpoint of the fiber yields a slight improvement to 81%. So this is unlikely to be helpful unless the dispersion is particularly small.

Another solution would be to have $\gamma_p = \gamma_i$, although this is not possible using the birefringent phase matching considered because of the reduction in the effective nonlinearity by a factor of 3 when the fields are orthogonally polarized. However if the nonlinear phase could be made factorable, a high purity could again be achieved with a large value of $\beta_{1s}L/\tau$.

B. Symmetric scheme

We now consider the symmetric scheme for avoiding correlations, with $\beta_{1s} = -\beta_{1i} = \beta_1$. This implies that $z_c = L - \frac{t_s - t_i}{2\beta_1}$ and $t_c = \frac{t_s + t_i}{2}$. Figure 5(a) shows the JTA in this case, where the temporal width τ of a Gaussian pump has been optimized to minimize correlation. Figure 5(b) shows the corresponding JSA without the effects of phase modulation, with R approaching zero, while Figure 5(c) shows the broadening and distortion from phase modulation when $R = 0.2$. Here, the broadening introduces spectral correlation, but it can be partly compensated by beginning with a longer pump pulse (increasing τ). Figure 6 shows the purity plotted against generation rate, both for a fixed value of β_1L/τ and with τ reoptimized as R is increased.

The predicted purities of around 80% here are somewhat low, even when R is kept small. A realistic experimental strategy may be to increase the purity above this by applying some spectral filtering to one photon of the pair, with transmission T defined as the probability of the filtered photon passing through the filtering. If the filtered photons are used as the heralds, the heralded photons will not experience any loss, just a reduction in effective generation rate, which is the product of R and T . Figure 7 shows the purity after one of the photons has been filtered with a top-hat transmission window of variable width as a function of RT . Five different values for the original generation R are shown, from 0.02 to 0.1. The purity initially rises rapidly as the filter removes the sinc ripples without too much attenuation (10%). However, we see a knee in the curve where filtering does not lead to great improvement without strong attenuation. The detrimental effect of phase modulation can be seen from the level of purity achievable before the knee, which falls as a function of R . However, for a given value of RT , a higher value of R still results in a higher purity.

Since a larger R appears to be beneficial for the purity after filtering, as a function of RT , this suggests there will be a trade-off between achieving higher purity and keeping multipair emission low, which occurs with probability approximately R^2 [21]. If photon-number-resolving detectors become available, they could be used on the heralds to detect and filter out multipairs. Otherwise, it may not be possible to simultaneously achieve a high-purity, highly effective generation rate and

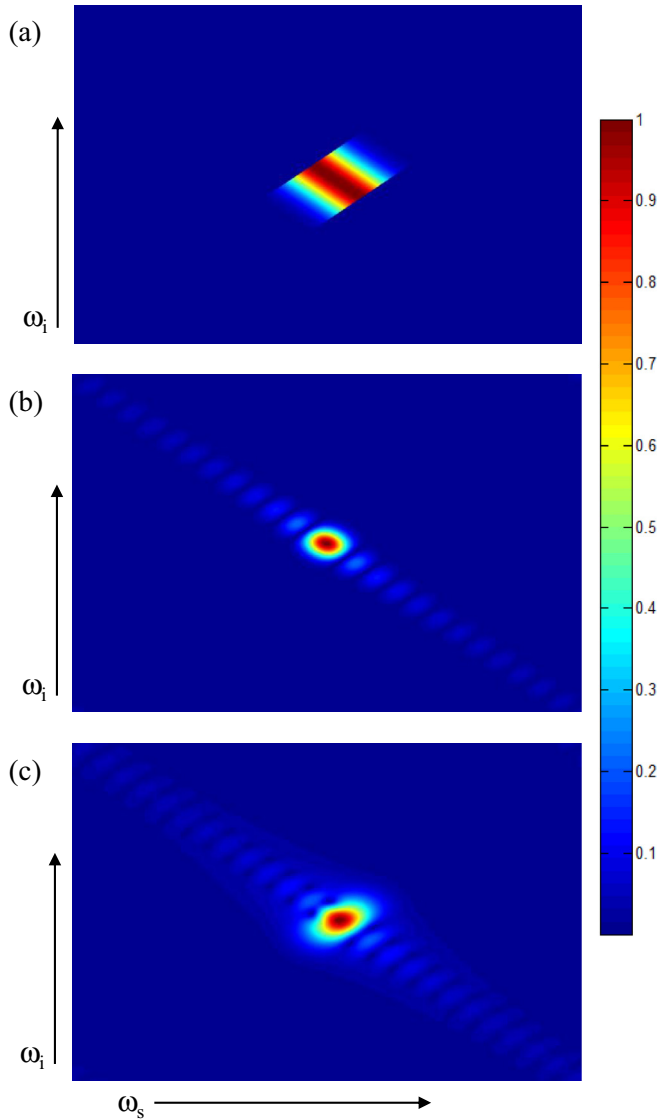


FIG. 5. (Color online) (a) Joint temporal amplitude when the signal and idler are equally spaced in β_1 about the pump. The pump duration is optimized to avoid correlation, but the hard edges to the JTA caused by the sudden beginning and end of the nonlinearity mean that some correlation is inevitable. (b) Corresponding JSA with a low generation rate. (c) Corresponding JSA at a higher generation rate, $R = 0.2$, showing the effects of SPM and XPM. The JSA is broadened in one direction.

low multipair emission using this scheme. In future work, it would be useful to consider similar schemes where two pump frequencies are used, with mismatched group velocities [27]. This can, in principle, remove the sinc ripples from the JSA and hence most of the correlation, although phase modulation may still have an effect.

V. NUMERICAL MODEL

To include the effects of group-velocity dispersion accurately, it is necessary to go to a numerical model involving finite steps along the fiber length. A common method for modeling the propagation of a laser pulse through a nonlinear

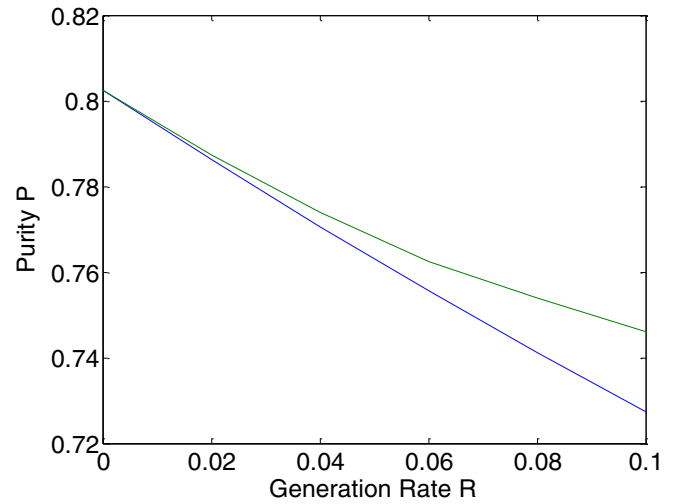


FIG. 6. (Color online) Purity against generation rate for the symmetric scheme. Blue (dark gray): τ is kept constant. Green (light gray): τ is increased with R to reoptimize. Again, the phase modulation reduces P as R is increased, although here P is lower to start with than in the asymmetric scheme because there is more correlation in the sinc ripples of the JSA.

and dispersive medium is a split-step Fourier (SSF) simulation [22]. Here, the length is divided into small steps Δz , and for each step, the nonlinearity and the dispersion are applied separately. For instance, the effect of propagating through the nonlinearity of Δz could be applied first, in the time domain where this is a simple calculation, then the pulse could be Fourier transformed to the frequency domain, where the effect of the dispersion can easily be applied using $\tilde{E}^+(z, \omega) = \tilde{E}^+(0, \omega)e^{ik(\omega)z}$, followed by inverse Fourier transform back to the time domain. Since the effects of the nonlinearity and dispersion are generally noncommuting, this is only approximate but is accurate for small Δz . In fact, it is better to

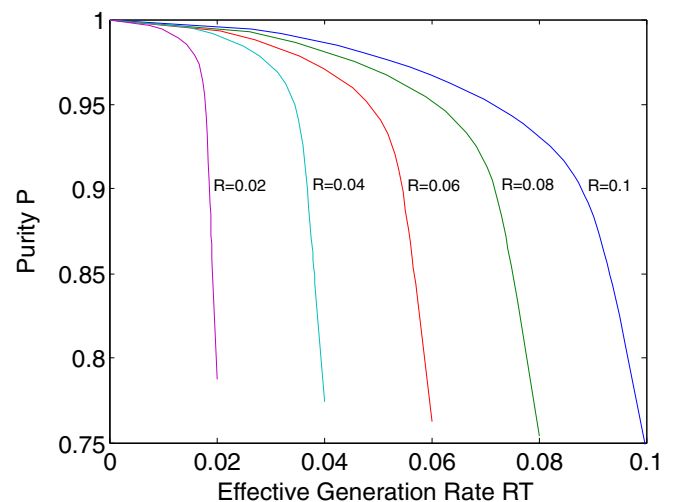


FIG. 7. (Color online) Purity as a function of the effective generation rate RT when filtering is applied to one of the photons (the herald) resulting in transmission T . Unfiltered generation rates R are shown from 0.02 to 0.1.

apply half a step of dispersion, then a full step of nonlinearity, followed by the other half step of dispersion because then the size of the errors due to the approximation varies with Δz^3 rather than Δz^2 [22].

To model the pair-production process along similar lines, we use a SSF simulation for the propagation of the pump pulse and incorporate spontaneous FWM into the nonlinear part of each step. The steps in position are kept small compared to the resolution in time, so that $\beta_{1s,i} \Delta z < \Delta t$. This means the signal and idler are initially in the same time bin as each other and as the component of the pump which created them, which simplifies the calculation for each step. To propagate the state of pairs created in previous steps, the half step of dispersion is applied to the JSA, which is then converted to a JTA by 2D Fourier transform so that XPM can be applied, before it is transformed back to a JSA for the next half step of dispersion. The state of the new pairs is coherently added for each step.

In the previous sections, the purity was determined by two parameters: the group velocities relative to the fiber length and pulse duration, $\beta_1 L / \tau$, and, when nonlinear phase modulation was taken into account, the total probability of pair generation R . Here, the group-velocity dispersions at each wavelength introduce additional relevant parameters: $\beta_2 L / \tau^2$ for the pump, signal, and idler. If the fiber length and pulse duration are increased in proportion, the effect of group-velocity dispersion decreases.

We again consider dispersion parameters taken from the birefringent microstructured fiber used in [25,26]. This fiber makes use of the asymmetric scheme to avoid correlations, with the pump pulse at 726 nm group velocity matched to the idler at 864 nm. The signal, phase matched at 626 nm, experiences walk-off with $\beta_{1s} = 1.14 \times 10^{-11} \text{ m}^{-1} \text{ s}$. The pump, signal, and idler experience group-velocity dispersion with $\beta_{2p} = 2.1 \times 10^{-26} \text{ m}^{-1} \text{ s}^2$, $\beta_{2s} = 3.6 \times 10^{-26} \text{ m}^{-1} \text{ s}^2$, and $\beta_{2i} = -1.3 \times 10^{-26} \text{ m}^{-1} \text{ s}^2$. The nonlinear parameters were estimated from the nonlinear refractive index of silica, approximately $2.7 \times 10^{-20} \text{ m}^2/\text{W}$, and the effective mode area, $3 \mu\text{m}^2$. Figure 8 shows the JSA produced from a 50-cm

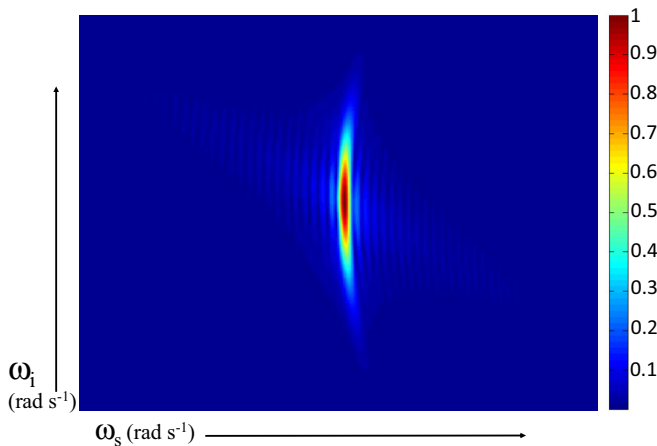


FIG. 8. (Color online) JSA from the numerical model including dispersion for realistic fiber parameters with a length of 50 cm and a pump bandwidth 2 nm. The dispersion causes some curvature of the JSA, which may introduce correlation.

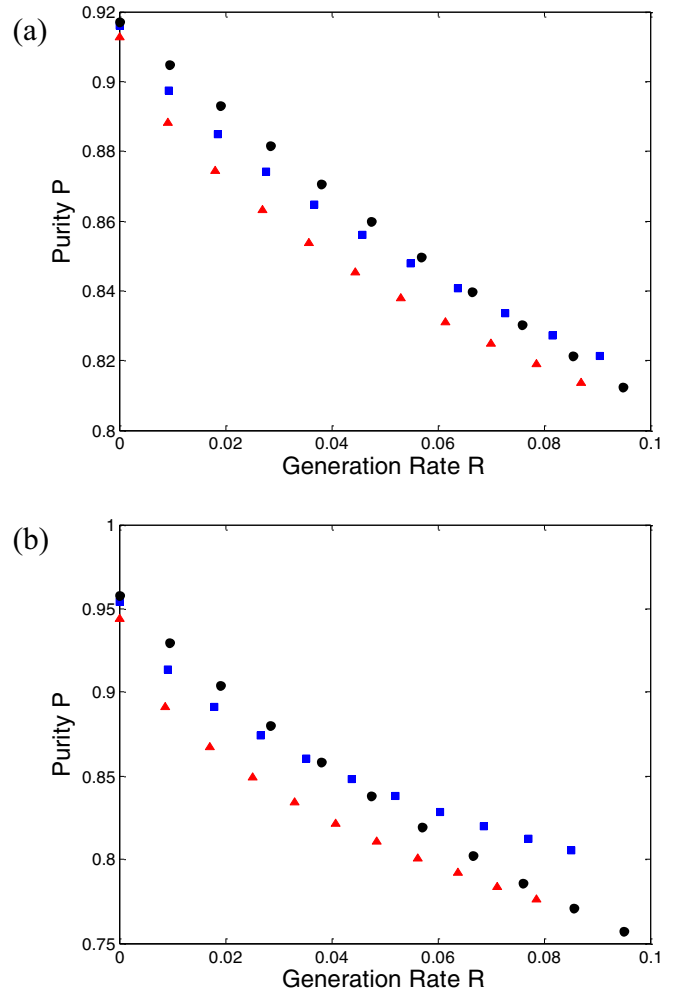


FIG. 9. (Color online) Purity against generation rate R for different strengths of dispersion, with an initial pump bandwidth of 1 nm. $R = 0$ corresponds to the case with no non-linear phase modulation. (a) $L = 0.5 \text{ m}$ and (b) $L = 1 \text{ m}$. In each case, black circles indicate no dispersion, blue squares show realistic dispersion, and red triangles illustrate double-strength dispersion. Surprisingly, at higher rates the dispersive case sometimes does better than the case with no dispersion.

fiber with a 2-nm initial pump bandwidth, corresponding to $\tau \approx 230 \text{ fs}$, and with the generation probability $R = 0.05$. The dispersion introduces some curvature to the JSA, so that it will become correlated for large bandwidth pulses.

In Fig. 9, the purity is plotted against the generation probability using the numerical model for different amounts of dispersion: no dispersion, dispersion using the realistic parameters, and double-strength dispersion. Physically, doubling the strength of the dispersion while keeping the other parameters constant could be achieved by halving the length of the fiber, halving the laser pulse duration, and adjusting the laser power to keep R constant. In Fig. 9(a), $\beta_{1s} L / \tau$ is approximately 12. It can be seen that for a very low generation rate, where phase modulation is negligible, the dispersion causes only a slight reduction in purity. The zero R intercept is close to our previous modeling results which ignore nonlinear phase modulation [15]. However, as R is increased, dispersion has a

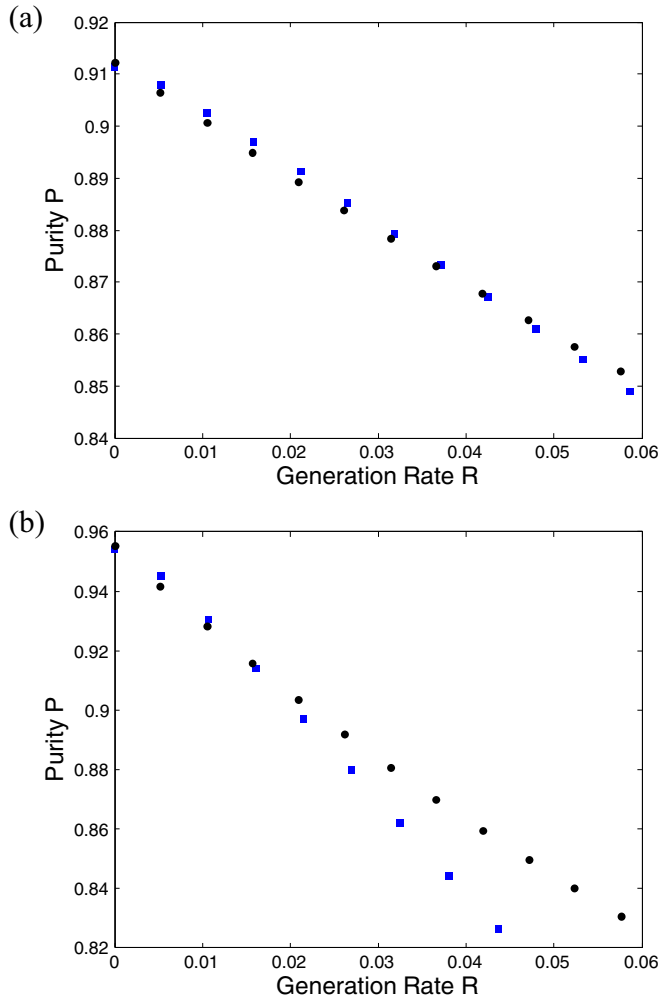


FIG. 10. (Color online) Purity against generation rate with anomalous dispersion for an initial pump bandwidth of 2 nm. (a) $L = 0.5$ m and (b) $L = 1$ m. In each case, black circles indicate no dispersion, and blue squares show realistic dispersion. Here, a very slight benefit can be seen at the low rate for the dispersive case compared to the case without dispersion.

larger effect, suggesting that dispersion and phase modulation are combining to create more of a reduction in purity than either would alone. Surprisingly, for higher values of R , this trend reverses, and the case with some dispersion actually does better than the case with no dispersion. This can be seen more prominently in Fig. 9(b), where the fiber length was doubled to 1 m, so that $\beta_{1s}L/\tau \approx 24$. It seems that for some choices of parameters, the nonlinear phase modulation and the dispersion begin to compensate one another, although here the effect is too small to change the trends seen before, with the purity still decreasing as the generation rate is increased and with a larger value of $\beta_{1s}L/\tau$ creating a better purity at a low rate but a worse purity at high rates.

Finally, we consider a different set of fiber parameters, corresponding to a birefringent microstructured fiber pumped at 1064 nm, in its anomalous dispersion region, generating phase-matched photons at 810 and 1550 nm [28]. The pump is polarized on the fast axis of the fiber, while the signal and idler are polarized on the slow axis, such that the signal is now

group velocity matched to the pump, while the idler walks off with $\beta_{1i} = 1.2 \times 10^{-11} \text{ m}^{-1} \text{ s}$. The dispersion parameters are $\beta_{2p} = -8.7 \times 10^{-27} \text{ m}^{-1} \text{ s}^2$, $\beta_{2s} = 1.0 \times 10^{-26} \text{ m}^{-1} \text{ s}^2$, and $\beta_{2i} = -6.4 \times 10^{-26} \text{ m}^{-1} \text{ s}^2$. Figure 10(a) shows the purity plotted against generation rate for a 50-cm length of this fiber with an initial pump bandwidth of 2 nm, resulting in $\beta_{1s}L/\tau \approx 12$, and Fig. 10(b) shows the case when the length is increased to 1 m, so $\beta_{1s}L/\tau \approx 24$. It can be seen that at low R , the dispersion improves the purity slightly compared to the case without dispersion but with phase modulation. However, for larger generation rates the combination of dispersion and phase modulation has a significant deleterious effect, as can be seen clearly in Fig. 10(b).

VI. CONCLUSION

We have seen that for schemes seeking to minimize the correlation between photon pairs generated by four-wave mixing, the effects of self-phase modulation and cross-phase modulation may be a limiting factor for the photons' purity which is not usually considered. For the asymmetric scheme, where one of the generated photons is group velocity matched to the pump pulse, it would otherwise be expected that, with a long interaction length and a wide pump bandwidth, very high purity could be achieved. However, when these additional nonlinear effects are included, the purity is degraded as the generation rate is increased, which may limit sources to low rates when a particular purity or quantum interference visibility is required. This can be seen both in an analytical model in the time domain, where group-velocity dispersion is neglected, and in a numerical model which includes both nonlinear effects and dispersion.

The symmetric scheme to generate pure photons is also considered, with the signal and idler group indices equally spaced above and below the pump group index. Again, the nonlinear effects significantly degrade the purity as the generation rate is increased, although here the main source of impurity is the correlation in the sinc ripples of the phase-matching function. These ripples can be eliminated with narrow filtering, but the purity only tends to unity as the transmission through the filter becomes small. In future work it would be interesting to consider the case with two pump fields at different wavelengths, where the sinc ripples can, in theory, be eliminated without filtering, but it seems likely that nonlinear effects will also be detrimental there.

The numerical model demonstrates that the impurities from nonlinear effects and from dispersion do not combine trivially, sometimes leaving a lower purity than would be expected when the effects are taken individually but in some regimes being slightly higher. It is possible that for particular choices of pump pulse power, duration, and shape, the effects of dispersion and nonlinearity could be made to cancel in a soliton-like manner and leave a high purity, although it is not expected that having the pump pulse alone propagating as a soliton would achieve this. It has also been shown that parametric gain can tend to equalize or lock group velocities, potentially leading to improved group-velocity matching in a dispersive medium [29].

We conclude that the discrepancy between previous modeling results and measured visibilities in heralded photon

interference experiments [13,15] can be largely explained by including nonlinear phase modulation. We also note that this effect limits the fidelity of cluster states generated by fusing entangled states [25,26] and thus could limit the scalability of cluster-state quantum computation based on FWM. This highlights a difference which has been overlooked between photon pair sources based on FWM in $\chi^{(3)}$ materials compared to SPDC in $\chi^{(2)}$ materials, where nonlinear phase modulation

is not present, and means that demonstrations of high purity in the latter cannot be expected to translate directly to the former.

ACKNOWLEDGMENTS

The authors acknowledge support from EU project 600838 QWAD and ERC advanced Grant No. 247462 QUOWSS.

-
- [1] N. Gisin and R. Thew, *Nat. Photonics* **1**, 165 (2007).
 - [2] T. D. Ladd, F. Jelezko, R. Laflamme, Y. Nakamura, C. Monroe, and J. L. O'Brien, *Nature (London)* **464**, 45 (2010).
 - [3] V. Giovannetti, S. Lloyd, and L. Maccone, *Nat. Photonics* **5**, 222 (2011).
 - [4] C. K. Hong, Z. Y. Ou, and L. Mandel, *Phys. Rev. Lett.* **59**, 2044 (1987).
 - [5] X.-S. Ma *et al.*, *Nature (London)* **489**, 269 (2012).
 - [6] J. L. O'Brien, G. J. Pryde, A. G. White, T. C. Ralph, and D. Branning, *Nature (London)* **426**, 264 (2003).
 - [7] S. Fasel, O. Alibart, S. Tanzilli, P. Baldi, A. Beverato, N. Gisin, and H. Zbinden, *New J. Phys.* **6**, 163 (2004).
 - [8] A. R. McMillan, J. Fulconis, M. Halder, C. Xiong, J. G. Rarity, and W. J. Wadsworth, *Opt. Express* **17**, 6156 (2009).
 - [9] X.-S. Ma, S. Zotter, J. Kofler, T. Jennewein, and A. Zeilinger, *Phys. Rev. A* **83**, 043814 (2011).
 - [10] M. J. Collins *et al.*, *Nat. Commun.* **4**, 2582 (2013).
 - [11] A. B. U'Ren, C. Silberhorn, K. Banaszek, I. A. Walmsley, R. Erdmann, W. P. Grice, and M. G. Raymer, *Laser Phys.* **15**, 146 (2005).
 - [12] P. J. Mosley, J. S. Lundeen, B. J. Smith, P. Wasylczyk, A. B. U'Ren, C. Silberhorn, and I. A. Walmsley, *Phys. Rev. Lett.* **100**, 133601 (2008).
 - [13] M. Halder, J. Fulconis, B. Cerny, A. Clark, C. Xiong, W. J. Wadsworth, and J. G. Rarity, *Opt. Express* **17**, 4670 (2009).
 - [14] O. Cohen, J. S. Lundeen, B. J. Smith, G. Puentes, P. J. Mosley, and I. A. Walmsley, *Phys. Rev. Lett.* **102**, 123603 (2009).
 - [15] A. Clark, B. Bell, J. Fulconis, M. M. Halder, B. Cerny, O. Alibart, C. Xiong, W. J. Wadsworth, and J. G. Rarity, *New J. Phys.* **13**, 065009 (2011).
 - [16] C. Söller, O. Cohen, B. J. Smith, I. A. Walmsley, and C. Silberhorn, *Phys. Rev. A* **83**, 031806 (2011).
 - [17] L. Cui, X. Li, and N. Zhao, *Phys. Rev. A* **85**, 023825 (2012).
 - [18] J. B. Spring *et al.*, *Opt. Express* **21**, 13522 (2013).
 - [19] L. G. Helt, M. J. Steel, and J. E. Sipe, *Appl. Phys. Lett.* **102**, 201106 (2013).
 - [20] W. P. Grice, A. B. U'Ren, and I. A. Walmsley, *Phys. Rev. A* **64**, 063815 (2001).
 - [21] P. J. Mosley, J. S. Lundeen, B. J. Smith, and I. A. Walmsley, *New J. Phys.* **10**, 093011 (2008).
 - [22] G. Agrawal, *Nonlinear Fiber Optics*, 5th ed. (Academic, Waltham, Massachusetts, US, 2012).
 - [23] B. Huttner, S. Serulnik, and Y. Ben-Aryeh, *Phys. Rev. A* **42**, 5594 (1990).
 - [24] A. Dot, E. Meyer-Scott, R. Ahmad, M. Rochette, and T. Jennewein, *Phys. Rev. A* **90**, 043808 (2014).
 - [25] M. S. Tame, B. A. Bell, C. DiFranco, W. J. Wadsworth, and J. G. Rarity, *Phys. Rev. Lett.* **113**, 200501 (2014).
 - [26] B. A. Bell, D. Markham, D. A. Herrera-Martí, A. Marin, W. J. Wadsworth, J. G. Rarity, and M. S. Tame, *Nat. Commun.* **5**, 5480 (2014).
 - [27] B. Fang, O. Cohen, J. B. Moreno, and V. O. Lorenz, *Opt. Express* **21**, 2707 (2013).
 - [28] A. R. McMillan, M. Delgado-Pinar, J. G. Rarity, and W. J. Wadsworth, *Proceedings of the International Quantum Electronics Conference and Conference on Lasers and Electro-Optics Pacific Rim 2011* (Optical Society of America, Massachusetts, 2011).
 - [29] N. Nasser, G. Fanjoux, E. Lantz, and T. Sylvestre, *J. Opt. Soc. Am. B* **28**, 2352 (2011).